International Journal of Scientific Engineering and Research (IJSER)
ISSN (Online): 2347-3878
Impact Factor (2024): 7.741

Remote Monitoring System for Gathering Information and Assessing Rainwater Quality

José de Jesús Moreno Vázquez [1], Aldo Rafael Sartorius Castellanos [2], Elsa Noemí Palomo Morales [3], Marcia Lorena Hernández Nieto [4], Antonia Zamudio Radilla [5]

[1, 2, 3, 4, 5] Tecnológico Nacional de México campus Instituto Tecnológico de Minatitlán, Departamento de Ingeniería Electrónica (The National Technological Institute of Mexico, campus Technological Institute of Minatitlán),
Av. Institutos Tecnológicos s/n Minatitlán, Veracruz, México
[1] *jose.mv[at]minatitlan.tecnm.mx*
[2] *aldo.sc[at]minatitlan.tecnm.mx*
[3] *elsa.pm[at]minatitlan.tecnm.mx*
[4] *marcia.hn[at]minatitlan.tecnm.mx*
[5] *antonia.zr[at]minatitlan.tecnm.mx*

Abstract: ***Acid rain, characterized by high concentrations of H_2SO_4, HNO_3, and H_2CO_3, is primarily caused by fuel combustion. It directly impacts plants, lakes, rivers, and human health, leading to an increase in respiratory conditions and cancer cases. This research focuses on characterizing precipitation by implementing a remote monitoring system for assessing rainwater quality. The system design utilized an ATMEGA 2560 microcontroller for signal processing and employed the Zigbee protocol to establish a wireless link. The main contribution of this research lies in the development of an electronic system for evaluating precipitation, specifically to measure the acidity or alkalinity of rainwater. The findings indicate that the information obtained from the system is accurate and valuable for determining the quality and potential uses of rainwater***

Keywords: Microcontroller, Zigbee, Water Quality, Remote Monitoring

1. Introduction

In large cities, industrialization and population growth directly affect the chemical composition of rainfall, leading to the generation of acid rain. Acid rain can be defined as any form of precipitation with high concentrations of sulfuric acid (H_2SO_4), nitric acid (HNO_3), and carbonic acid ($H2CO_3$). The presence of sulfur dioxide (SO_2) is primarily attributed to the combustion of fossil fuels and factors such as the incineration of organic matter. SO_2 undergoes immediate oxidation and upon contact with water, converts into H_2SO_4. Similarly, nitrogen dioxide can convert into nitric acid in the atmosphere. These acids serve as the primary precursors of acid rain [1], [2]. Under natural conditions, acid deposition has an approximate pH value of 5.6, owing to the presence of carbonic acid in small quantities in the atmosphere. Acid rain occurs when rainwater registers a pH value lower than 5.6. Although it does not directly impact ecosystems, acid rain has the potential of reducing biodiversity and removing essential nutrients for plant growth or agricultural crops [3]–[5]. Additionally, acid rain can cause deterioration of constructions or metallic materials.

Considering that most of the planet is composed of water, with nearly 97% being salt water, and acknowledging water as a non-renewable natural resource, the supply of rainwater becomes increasingly significant. However, Mexican regulations establish permissible quality limits to which drinking water must adhere to prevent various diseases such as gastrointestinal issues [6].

Today, there are numerous instruments available for measuring precipitation, with notable examples including the cup rain gauge, current meter, and weighing rain gauge. In the current meter, collected water flows into a container equipped with a float. As the water level rises, the float undergoes vertical movement, locking a diagram that represents the accumulation of water in the container over time. This resulting graph is referred to as a hyetograph. By analyzing the slope of the hyetograph, we can calculate the intensity of the rainfall [7]. The weighing rain gauge is particularly recommended for cold climates, as it is capable of recording various types of precipitation including rain, hail, or snow. Its operation relies on a system of weights or springs [8]. The cup rain gauge is the most common instrument used for measuring liquid precipitation. It functions by collecting rainwater through a funnel and directing it into two containers that are unbalanced, causing a balancing movement each time rainwater is collected. This tilt of the scale can be utilized to generate a frequency, converting the mechanical motion into an electrical signal that can be manipulated to activate an electronic device.

When measuring hydrogen potential, temperature serves as a crucial physical parameter that can influence the accuracy of pH readings. This is because temperature variations can occur between the sample and the buffer solutions used to calibrate the pH electrode, leading to deviations in pH measurements. To address this issue, various temperature sensors are commonly employed for recording temperature.
Resistive temperature detectors (RTDs) operate based on the variation of the resistance of a conductor with temperature. The resistance of RTDs is directly proportional to the amount of incident light upon them. Semiconductor temperature sensors offer greater precision, better linearity, compact size, and improved stability compared to RTDs. Thermocouples, another type of temperature sensor, are composed of two different metals joined together to form a junction. This junction produces a voltage, which varies according to the temperature difference between the "hot point" or measurement point and the "cold point" or reference point [9]. Currently, there are technological methods used to carry out the pH measurement process in a

substance, and we can classify them into two groups: electrochemical and optical. Electrochemical sensors are those that convert the activity of the hydrogen ion into an electrical signal. Within this type of transducer, we can find Ion Selective Electrodes (ISE) and Ion Sensitive Field Effect Transistors (ISFET). Optical sensors are divided into colorimeters or reagent strips for pH measurement, and fiber optic sensors [10].

In modern times, numerous researchers have designed systems for monitoring meteorological variables [11]–[13]. Not all research groups focus on measuring the acidity of precipitation, especially considering the high cost of existing equipment. Presently, the Environmental Engineering Department of the Technological Institute of Minatitlán is conducting research to assess rainwater quality. However, the current method used does not offer simultaneous and real-time data on the acidity or alkalinity of rainfall. Thus, this article introduces the design of a remote monitoring system to characterize these variables, aiming to provide essential information for determining rainwater quality and its potential uses. The proposed system primarily targets environmental researchers and involves the acquisition and processing of signals, which will be transmitted wirelessly to a computer and stored in a database. This data will then be accessible to any interested user. It's worth noting that one of the primary objectives of this research is to enhance the recording technique for these variables. Currently, the method relies on field measurements, and at times, samples must be transferred to the laboratory for analysis. This process often leads to inaccuracies due to the time gap between the event and the measurement, highlighting the need for improvement.

2. Material

The architecture employed for designing the temperature, precipitation, and rainfall acidity monitoring system is illustrated in the block diagram shown in Figure 1. This diagram depicts the transmission scheme utilized for wireless communication.

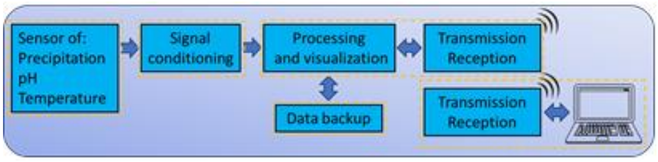

Figure 1: Block diagram of the remote monitoring system

We utilized a Davis 7852M tipping bucket rain gauge with a resolution of 0.254mm for rainfall assessment. This device, featuring a contact closure output and a collection area of 214 cm^2, conforms to the specific standards established by the World Meteorological Organization. It was calibrated upon acquisition and was further adapted for signal processing through the integration of relevant electronic instrumentation. For temperature measurement, we employed a DS18B20 model programmable resolution digital sensor. This sensor utilizes the 1-Wire communication protocol and allows for resolution selection ranging from 9 to 12 bits. With a measuring range of -55 °C to 125°C and an accuracy of ±0.5°C within the range of -10 °C to 85 °C, it proved to be suitable for our needs. It is important to note that, due to the T0-92 type encapsulation of the DS18B20 temperature sensor, precautions were taken to insulate the sensor pins to prevent direct contact with water. This was achieved by encasing the sensor pins in epoxy resin and placing them within a plastic tube, leaving only the pure encapsulation exposed.

Figure 2: DS18B20 Temperature Sensor with Liquid Isolation.

The hydrogen potential (pH) recording was conducted using a combined pH electrode, similar to the one depicted in Figure 3A. This electrode transmits a signal in millivolts to an acquisition card, as illustrated in Figure 3B, for characterization and subsequent transmission to the processing stage to ensure accurate assessment.

The measurement kit offers a pH measurement range from 0.01 to 14, utilizing the RS-232 communication protocol. Additionally, it is capable of providing pH readings with reference to a desired temperature.

A) B)

Figure 3: A) Combined glass electrode used for pH measurement. B) Data acquisition card.

To process signals obtained from signal conditioning, we employed an Arduino MEGA R3 electronic board, which incorporates an ATMEGA2560 microcontroller. The wireless connection between the sensor module and the computing equipment was established using Xbee radios, which utilize the ZigBee communication protocol. These radios operate in the 900MHz ISM band and have an urban range of 370 meters.

The user interface implemented in the signal processing module is managed by a 2.8-inch resistive touchscreen display.

3. Methods

Precipitation is typically measured in mm. This unit is chosen because if one liter of water were poured onto a completely flat horizontal surface of 1 square meter, the thickness of the water layer would be 1 mm. The inside of the rain gauge is depicted in Figure 4. The Davis 7852M tipping bucket rain gauge, with a resolution of 0.254

millimeters, operates by generating a specific frequency based on the amount of water recorded.

The volume of water required to tip the buckets is determined by the collection area of the rain gauge and its resolution. Therefore, the calculation is as follows:

$$214\ cm^2 \times 0.0254\ cm = 5.4356\ cm^3 = 5{,}4356\ ml. \quad (1)$$

Figure 4: Interior of the rain gauge

Therefore, according to the calculations performed, when one bucket is filled, it releases an approximate 5.4ml of liquid each time an internal movement occurs. This amount of water is equivalent to the 0.254mm resolution specified in the equipment's datasheet.

It is important to note that the system tests were conducted in a laboratory setting. To obtain precipitation sensor readings, various amounts of water were poured into the rain gauge using a graduated cylinder. However, potential deviations observed in the sensor readings compared to the graduated cylinder are influenced by the conditions under which the measurements were taken. Factors such as the speed at which the liquid is poured into the rain gauge and the location where the water stream falls in relation to the center of the rain gauge can alter the measurement due to the lack of the same heterogeneity present in real rainfall conditions.

To observe the discrepancy between the true value and the measured value by the system, the error was determined – the difference between the measured value and the real value. However, it is common to express the error as the ratio of the absolute error to the true value, expressed as a percentage. Nevertheless, for this case, the sign of the error is retained.

The pH meter used was calibrated on day 1, five minutes before the commencement of measurements, to evaluate our instrument against a standard device. For this process, it is only necessary to send commands to the pH acquisition card, which will return the format XX.XX<CR>, depending on the command sent. The calibration process is outlined below:

1) Carefully rinse the pH electrode with distilled water.
2) Immerse the pH electrode in the pH 7 buffer solution.
3) Wait approximately 1 to 2 minutes and press the pH 7 button displayed on the screen.
4) Rinse the electrode thoroughly with distilled water and dry it with a lint-free dry towel.
5) Immerse the pH electrode in the pH 4 buffer solution.
6) Wait approximately 1 to 2 minutes and press the pH 4 button displayed on the screen.
7) Rinse the electrode thoroughly with distilled water and dry it with a lint-free dry towel.
8) Immerse the pH electrode in the pH 10 buffer solution.
9) Wait approximately 1 to 2 minutes and press the pH 10 button displayed on the screen.
10) Now, simply press the Stop button on the screen, rinse the electrode thoroughly with distilled water, and clean it with a lint-free towel. The electrode is now calibrated.

Once the calibration steps and methods for recording precipitation, temperature, and rainfall acidity are defined, it is important to clarify the system's operation in its wireless transmission mode. The system is designed to record temperature and pH every 10 seconds while waiting for the acidity variation of the rainwater to stabilize at a pH greater than or equal to 5.6 before changing the sampling time to 10 minutes.

Given that the tests conducted to evaluate the implemented system utilized a single water sample, and the temperature was assessed under similar conditions for all three days, it was decided to obtain the daily average of the samples and their standard deviation. This approach allows observing the variations in the results of the developed system concerning the pH meter model 8689, which also records the temperature of the study sample.

4. Results

The results presented stem from the analysis of different water samples over a period of 3 days, aimed at determining the repeatability of the temperature sensors and the pH electrode. Additionally, the objective is to observe the variation and accuracy of the results as the days progress, considering that the electrode was calibrated only on day 1 of the experiment. Tables 1 and 2 display the average and standard deviation results of the samples taken with the reference instrument and the implemented system.

Table 1 outlines the variations in pH samples compared to a standard record. On day 1, considerable fluctuations in the measurement were observed, as indicated by the standard deviation of the sample. However, the mean obtained with the implemented pH meter demonstrates acceptable accuracy compared to the standard sample, considering an approximate measurement error of ±0.5.

Significant variation compared to the standard measurement was observed by the third day, where it is detailed that the average of the sample obtained with the implemented pH meter already shows a variation of approximately 0.3 compared to the reference pH meter. It is crucial to note that while there appears to be more stability in the measurements on days 2 and 3, the readings recorded by the system no longer exhibit the same accuracy as the measurements on day 1.

Table 1: Results table of pH measurements taken with the designed system and the pH Meter 8689.

Day	pH pattern data sample	Developed pH system
1	7.416±0.040	7.431±0.147
2	7.391±0.041	7.558±0.042
3	7.330±0.031	7.629±0.080

The information presented in Table 2 pertains to the records obtained from readings taken with the DS18B20 temperature sensor, using the temperature displayed by the pH Meter 8689 as the measurement reference. It is observed that the temperature sensor exhibits good accuracy and precision relative to the measurement considered as the standard.

In Table 3, the data obtained from the Davis rain gauge is presented, revealing deviations compared to the standard instrument, with observed errors of up to 4%.

Table 2: Temperature results table taken from the pH Meter 8689 and the DS18B20 sensor.

Day	*pH pattern data sample*	*Developed pH system*
1	25.223±0.110	25.124±0.106
2	23.8±0.0692	23.749±0.061
3	25.173±0.087	25.170±0.298

Table 3: Results obtained from the Davis 7852M rain gauge.

Test Tube (ml)	*Davis rain gauge (ml)*	*Error (%)*
40	39	-2.50
50	52	4
60	58	-3.33
70	69	-1.42
80	76	-5
90	91	1.11
100	101	1
150	146	-2.66
200	193	-3.50
250	253	1.20
300	293	-2.33
350	351	0.28
400	391	-2.25
450	450	0
500	496	-0.80

Figure 5 illustrates the initial startup window of the system, prompting the user to first install the driver for the computer to recognize the USB device to be connected, in this case, the XBee radio. The second point to address is port recognition, where the port number occupied by the USB device is stored in the database. The purpose of this option is to enable the system to automatically recognize the device each time it is connected or disconnected. Step 3, port registration, is solely used to save the recognized port. The fourth step in software installation is the start button for initiating the system installation process on the computer.

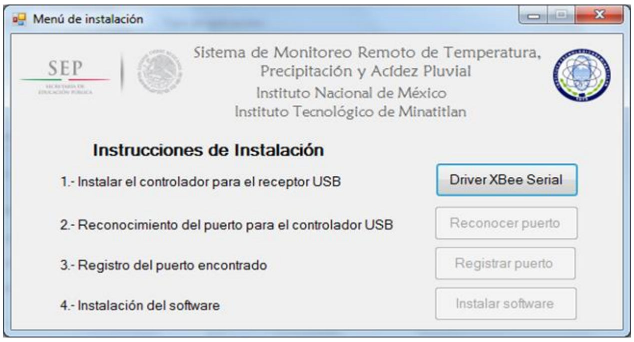

Figure 5: Initial installation screen. The screen shows the installation steps when an XBee radio is connected

In Figure 6, the main screen of the implemented software is displayed. The screen presents remotely recorded data, including the registration time and date. Additionally, there is a button for accessing the log history, and a list is included showing the node number from which the sample is taken.

Figure 7 shows a front view of the equipment for data acquisition and represents the final prototype of the developed node. In it, connectors such as the RJ-11, serving as the input for the rainfall sensor, can be observed. The Molex connector is linked to the DS18B20 temperature sensor, and a BNC input is available for the pH electrode. Additionally, there is the presence of a resistive TFT touch screen display.

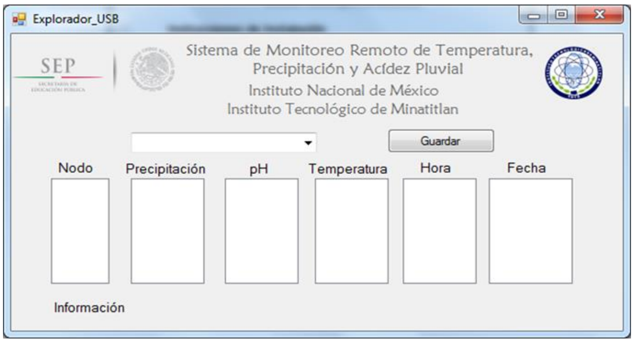

Figure 6: Main screen of the monitoring system. The screen displays variables obtained from the field modules, along with the time and date when the data are received.

Figure 7: Final hardware, front view.

Figure 8 showcases the casing supporting the various sensors implemented in the system, along with the equipment responsible for processing the obtained signals. The designed structure features a front door and a top cover. To prevent sample overheating, the casing was painted with two layers of white enamel. The lower part of the frame is covered to prevent sample contamination. Additionally, an opening is visible on the top cover, serving as the emergence point for the funnel of the rain gauge.

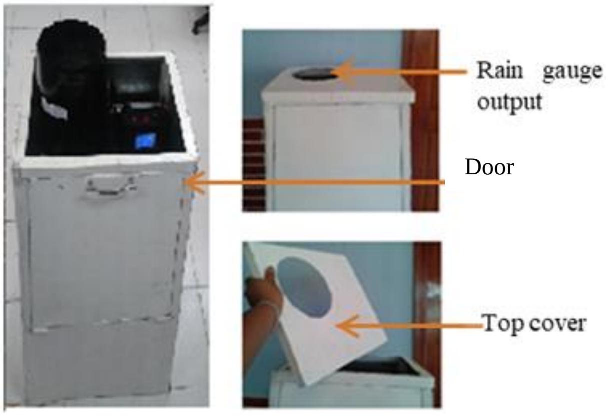

Figure 8: Prototype Enclosure Structure

Figure 9 illustrates the arrangement of the signal processing system. In the figure, the Davis 7852M rain gauge is visible, along with the hoses used to guide the collected liquid to the container holding the sample. Additionally, the pH measuring electrode and the DS18B20 temperature sensor are observed, both secured to the structure by a metal filament.

Figure 9: Interior of the casing with sensors and the data processing system

5. Discussion

The recording of rainfall can be accomplished through various systems. In some cases, sensors record both solid and liquid precipitation, while other instruments measure the amount of water falling using a graphical representation [14]–[16]. Unlike weather radar, cup-type rain gauges measure the total water fallen in a specific area, allowing the sample to be emptied from the instrument through lower openings. For this research, a cup-type rain gauge was chosen, considering its self-emptying feature. However, potential errors such as accidental tilt, absence of measurements for weak precipitation, variations in sample shape, and interference from strong winds needed to be addressed [17],[18].

The cup-type rain gauge was considered the optimal choice for determining the amount of precipitation, especially when measuring liquid precipitation. While some researchers have designed and constructed such instruments, for this study, purchasing a pre-calibrated sensor was preferred. This ensured accurate measurements without the need for prior adjustment, except for proper leveling during installation.

During the validation of the cup rain gauge, laboratory tests revealed errors in the measurement of rainfall that may vary compared to the results obtained under real conditions [19], [20]. Although laboratory testing was consistent with this study, it is highly recommended to validate the system using a similar instrument or a conventional weather station. This is because the 30% error observed in comparison to a graduated cylinder may vary with real-world measurements.
The characterization of hydrogen potential is crucial for evaluating the acidity or alkalinity levels of rainwater. Under normal conditions, rainwater typically tends toward a pH value of 5.6, influenced by atmospheric carbonic acid. Any deviation from this value is primarily attributed to atmospheric emissions of various origins, with the combustion byproducts of fossil fuels being a significant source of pollution [3], [21]. Despite efforts to reduce dust and smoke emissions, gases released into the atmosphere contribute to phenomena like acid rain or global warming. All forms of ambient water, including snow, ice, and fog, contain carbon dioxide. Consequently, water is somewhat acidic, with a pH of about 5.6, but acid rain has a pH of 5.0 and can occasionally reach a pH of 3 [22], [23].

There are several methods to measure the pH of a liquid, with one of the most common being electrochemical [24]. The electrochemical method operates similarly to a cell, referencing two electrodes, one with a constant pH and the other with the unknown pH of the sample. This research aims to evaluate rainwater pH to provide a record for qualified personnel to determine water potability. Numerous studies have focused on determining hydrogen potential to assess the acidity of water or other solutions [25]–[27].

The combined electrode is one of the most commonly used instruments for pH measurement. However, there are also ion-sensitive field-effect transistors (ISFETs), which function similarly to a MOS transistor. Although ISFETs are smaller and light-sensitive, their thermal instability necessitates operation at a constant temperature for accurate results [28]. Several studies have presented specific models of ISFET sensors, where it is observed that they have a wide working range with respect to temperature. However, the pH range measured is typically from 2 to 12, with a response time greater than that of the glass electrode. Nevertheless, their availability in the market and the limited pH measurement range they offer sometimes result in their use being discarded [10].

The electrochemical method relies on measuring the potential difference between electrodes. Some sensors incorporate two electrodes: a reference electrode and another to measure the sample, known as combined electrodes, where only the potential generated in millivolts is measured to determine the pH value by signal conditioning. There are ongoing efforts in which the design of the signal conditioning stage for pH measurement is being developed [29], [30]. However, the design of the conditioning stage must take into account the pH measurement range desired, as sometimes it is only designed for a specific range, making a 10-bit converter sufficient. However, the design of the conditioning stage must take into account the desired pH measurement range, as sometimes it is only designed for a specific range, making a 10-bit converter sufficient. However, in the development of this work, a pH ranges from 0 to 14 was required because, in the future, it is also intended to measure the potability of water with pH values between 6.5 and 8.5 [31]. Therefore, the internal analog-to-digital converter of the ATMega2560 microcontroller was not used. Instead, an interface to the pH sensor was employed (Figure 3). The interface is similar to that used by other authors [16], [32], [33].

An important consideration when acquiring pH data is temperature. Theoretically, when measuring a pH of 7 at 25°C, the sensor should output 0 V and generate increments of approximately ±59.2 mV per pH unit [34]. However, calculations conducted at different temperatures reveal that the sensor's response per pH unit may vary with the recorded temperature [35]. For measurement purposes, temperature compensation is necessary. This procedure can be done digitally (obtaining the temperature and adjusting the value by software) or analogically by adjusting the temperature together with the pH before being sent to an A/D converter as shown by other authors in different areas [29], [31], [36]. There are several low-cost sensors for temperature measurement. Although some authors indicate that the sensor is of high cost [37]. In this work, the DS18B20 was selected as it is one of the most widely used sensors [16], [38], [39]. Additionally, using a single bit to communicate optimizes the use of the microcontroller's input-output ports, unlike others that use SPI (Serial Peripheral Interface) and require more bits of the microcontroller port and even signal conditioning for analog sensors such as the LM35.

On the other hand, there are systems that monitor water quality in general [33], [40]–[42], but they do not measure the quantity and acidity of rainwater specifically to determine the impact of contamination in the area being monitored. Therefore, the developed work measures the total amount of water dropped and the pH of the water in relation to its temperature. The records obtained are stored directly on a MicroSD memory as a backup in case data transmission cannot be performed. When data transmission between the node and the server is completed, the backup information of the slave node is deleted. The wireless transmission method used is polling.

Information transmission between two stations or nodes can be accomplished using various communication technologies. There are works where the Ethernet standard was employed for transmitting information generated by ISFET sensors [43]–[45]. However, implementing this scheme requires a physical connection to a controller for handling the generated records. Other methods for data communication could involve LoRa [46], Global System for Mobile Communications (GSM) [47], [48], specifically the Short Message Service (SMS) function [49], Although studies already exist for transmitting meteorological variable records, it's worth mentioning that sending text messages incurs a cost per SMS, and it's restricted to 160 characters per SMS [50]. Additionally, utilizing IoT based on mobile telephony incurs a cost for utilizing the provider's network. Another option is through the use of Bluetooth, albeit with a shorter range [16], [46], [51]. The utilization of the Internet of Things (IoT) is experiencing a significant rise in data transfer. However, as mentioned, not only is there a network access fee, but there are also situations where transmitting information via the internet is challenging [52]. Therefore, other forms of wireless communication are required or combining different communication schemes with IoT through ZigBee, as demonstrated by some authors [16], [45], [53].

Hence, the use of Wi-Fi could be an alternative. Although it has a range of 100 meters [30], it still has limited coverage for the area where the system was tested at the Technological Institute. Therefore, the choice was made to use the ZigBee standard operating under an XBee device in the free frequency around 900 MHz [16]. It's more suitable for transmitting the records generated by the hardware, as the range can be up to 370 meters in urban areas. The use of XBee modules with a frequency of 900 MHz is because lower frequency results in longer wavelengths, meaning greater distance but lesser data transmission [54]. For the specific case of this work, a short-range link covering a minimum range of 700 meters was required, and considering the characteristics of the device to be used, it could offer up to 24 kilometers in line of sight using a high-gain antenna [55]. For testing purposes of the developed system, a dipole antenna in an urban range with a coverage of approximately 100 meters was used. If a greater range were required, as mentioned, it could be achieved using a high-gain antenna.

6. Conclusions

A remote monitoring system was implemented, which takes constant readings every 10 seconds until the precipitation reaches a pH of 5.6. Once this value is reached, the system takes samples every 10 minutes. This data record is utilized by environmental experts for decision-making purposes, aiming to assess the acidity level of rainwater to evaluate its quality. The instruments employed in the research are part of a study conducted on various sensors, where it was observed that the application of a tipping bucket rain gauge with a resolution of 0.254 mm for recording rainfall was suitable, along with a combined electrode for pH measurement across its entire scale, ranging from 0 to 14 pH. Additionally, a solid-state sensor model DS18B20 was considered for temperature evaluation; however, it was necessary to adapt this transducer for immersion in water. Daily inspection of the instruments is necessary to prevent blockage, especially in the case of the rain gauge, and calibration of the electrode at least once a day is required to obtain more precise and accurate data. The tipping bucket rain gauge is an instrument that, through mechanical action, provides a frequency. Therefore, to avoid noise, an RC filter was implemented with an oscillation not exceeding 5 hundredths of a second, taking into account that the opening and closing of the reed switch oscillate between 40 and 100 milliseconds. The main advantage of the temperature sensor is that it provides samples in digital format, and it was only necessary to place a resistor as indicated in the datasheet. However, an inconvenience that could arise in the electrode acquisition card is any modification of characters in the card's programming for sensor calibration as well as for accessing the results obtained by the sensor. The Arduino Mega electronic board hosts an 8-bit microcontroller, which was considered necessary because the pH acquisition card already yields a processed result. However, if a more detailed study in pH acquisition were desired, it would be advisable to use a 32-bit microcontroller to evaluate the pH acquisition time between one design and another, as well as to observe the advantages it offers in terms of transmission speed and information display on the screen.

References

[1] D. Granados Sánchez, G. F. López Ríos, y M. Á. Hernández García, «La lluvia ácida y los ecosistemas forestales», Rev. Chapingo Ser. Cienc. For. Ambiente, vol. 16, n.o 2, pp. 187-206, dic. 2010, doi: 10.5154/r.rchscfa.2010.04.022.

[2] P. D. Carrera Oscullo, L. S. Vaca Álvarez, E. O. Segura Chávez, y M. A. Taco Ugsha, «Análisis de lluvia ácida en la ciudad de Nueva Loja, provincia de Sucumbíos», Green World J., vol. 4, n.o 3, p. 002, dic. 2021, doi: 10.53313/gwj43002.

[3] Secretaría del Medio Ambiente de la Ciudad y de México, SEDEMA, «Calidad del aire en la Ciudad de México, Informe anual 2020.» Dirección General de Calidad del Aire, Dirección de Monitoreo de Calidad del Aire., 2023.

[4] M. I. H. Zaidi Farouk, Z. Jamil, y M. F. Abdul Latip, «Towards online surface water quality monitoring technology: A review», Environ. Res., vol. 238, p. 117147, dic. 2023, doi: 10.1016/j.envres.2023.11714.

[5] R. Qu y G. Han, «A critical review of the variation in rainwater acidity in 24 Chinese cities during 1982–2018», Elem. Sci. Anthr., vol. 9, n.o 1, ene. 2021, doi: 10.1525/elementa.2021.00142.

[6] R. J. Alvarez, «01-18-96 NORMA Oficial Mexicana NOM-127-SSA1-1994, Salud ambiental, agua para uso y consumo humano-Límites permisibles de calidad y tratamientos a que debe someterse el agua para su potabilización».

[7] F. J. S. S. Román, Hidrología Superficial y Subterránea. 2022.

[8] Ideam, Invemar, «Protocolo de Monitoreo y Seguimiento del Agua.» Bogotá, D. C., 2021.

[9] J. Liu, L. Ma, y J. Yang, «Methods and techniques of temperature measurement», en 2011 International Conference on Electrical and Control Engineering, sep. 2011, pp. 5332-5334. doi: 10.1109/ICECENG.2011.6057907.

[10] S. Sinha y T. Pal, «A comprehensive review of FET-based pH sensors: materials, fabrication technologies, and modeling», Electrochem. Sci. Adv., vol. 2, n.o 5, p. e2100147, 2022, doi: 10.1002/elsa.202100147.

[11] R. O. Domínguez-García, Y. Aguilar-Molina, J. Y. Rumbo-Morales, F. Sorcia-Vázquez, G. Ortiz-Torres, y M. González-Dueñas, «Diseño e implementación de un dispositivo de Internet de las Cosas para el monitoreo del medio ambiente vía Wi-Fi - RIIIT». [Online]. Available at: https://riiit.com.mx/apps/site/idem.php?module=Catalog&action=ViewItem&item_id=85426

[12] O. A. Adenekan, M. A. Sodunke, A. I. Olateju, y O. Bello, «Weather Variables Monitoring System with A Developed Graphical User Interface Using Internet of Thing», Int. J. Innov. Eng. Res. Technol., vol. 8, n.o 3, pp. 55-65, 2021.

[13] G. M. Vega, «Desarrollo de un sistema de monitoreo meteorológico de bajo costo basado en tecnología IoT.», dic. 2023. [Online]. Available at: https://ring.uaq.mx/handle/123456789/9793

[14] R. Morbidelli, Ed., Rainfall: Modeling, Measurement and Applications. Amsterdam Kidlington, Oxford Cambridge, MA, 2022.

[15] A. Bracci et al., «Quantitative Precipitation Estimation over Antarctica Using Different Ze-SR Relationships Based on Snowfall Classification Combining Ground Observations», Remote Sens., vol. 14, n.o 1, Art. n.o 1, ene. 2022, doi: 10.3390/rs14010082.

[16] F. Jan, N. Min-Allah, y D. Düştegör, «IoT Based Smart Water Quality Monitoring: Recent Techniques, Trends and Challenges for Domestic Applications», Water, vol. 13, n.o 13, Art. n.o 13, ene. 2021, doi: 10.3390/w13131729.

[17] E. Ml, «Techniques of Filling Missing Values of Daily and Monthly Rain Fall Data: A Review», CienceForecast Publ. LLC, vol. 3, 2020.

[18] A. Cauteruccio, M. Colli, M. Stagnaro, L. G. Lanza, y E. Vuerich, «In-situ Precipitation Measurements», en Springer Handbook of Atmospheric Measurements, T. Foken, Ed., en Springer Handbooks. , Cham: Springer International Publishing, 2021, pp. 359-400. doi: 10.1007/978-3-030-52171-4_12.

[19] L. G. Lanza et al., «Calibration of non-catching precipitation measurement instruments: A review», Meteorol. Appl., vol. 28, n.o 3, p. e2002, 2021, doi: 10.1002/met.2002.

[20] D. A. Segovia Cardozo y L. Rodríguez Sinobas, «Método para la corrección de errores de medición causados por la intensidad de precipitación en pluviómetros de cazoletas basculantes», ES2831899B2, 01 de 2022 [Online]. Available at: http://www.oepm.es/pdf/ES/0000/000/02/83/18/ES-831899_B2.pdf

[21] C. Pulido Valero y J. R. Cano, «Análisis comparativo de las condiciones de acidez de la precipitación y el contexto meteorológico relacionado con el fenómeno, en las localidades de Chapinero, Usaquén y La Candelaria, ubicadas al oriente de la ciudad de Bogotá D.C», Ing. Ambient. Sanit., ene. 2021, [Online]. Available at: https://ciencia.lasalle.edu.co/ing_ambiental_sanitaria/1903

[22] N. J. Calixto, D. Becerra Moreno, y J. A. Cárdenas-Gutiérrez, Causas y consecuencias de la contaminación de aguas. Bogotá - Ediciones Nueva Jurídica, 2023. [Online]. Available at: https://repositorio.ufps.edu.co/handle/ufps/6720

[23] H. O. T. Pye et al., «The acidity of atmospheric particles and clouds», Atmospheric Chem. Phys., vol. 20, n.o 8, pp. 4809-4888, abr. 2020, doi: 10.5194/acp-20-4809-2020.

[24] L. Manjakkal, D. Szwagierczak, y R. Dahiya, «Metal oxides based electrochemical pH sensors: Current progress and future perspectives», Prog. Mater. Sci.,

vol. 109, p. 100635, abr. 2020, doi: 10.1016/j.pmatsci.2019.100635.

[25] K. B. Gomez Moscoso y S. H. Vizcarra Medina, «Aplicación de sistema de información geográfica en la recuperación de aguas contaminadas, Revisión Sistemática: 2015-2021», Repos. Inst. - UCV, 2023, [Online]. Available at: https://repositorio.ucv.edu.pe/handle/20.500.12692/113334

[26] Z. Zhou, Z. Pei, L. Wei, S. Zhao, X. Jian, y Y. Chen, «Electrocatalytic hydrogen evolution under neutral pH conditions: current understandings, recent advances, and future prospects», Energy Environ. Sci., vol. 13, n.o 10, pp. 3185-3206, doi: 10.1039/D0EE01856B.

[27] D. R. Nayar, «Assessment of Water Quality Index and Monitoring of Pollutants by Physico-Chemical Analysis in Water Bodies: A Review», Int. J. Eng. Res. Technol., vol. 9, n.o 1, ene. 2020, doi: 10.17577/IJERTV9IS010046.

[28] W. Xiao y Q. Dong, «The Recent Advances in Bulk and Microfluidic-Based pH Sensing and Its Applications», Catalysts, vol. 12, n.o 10, Art. n.o 10, oct. 2022, doi: 10.3390/catal12101124.

[29] E. J. Á. Rodríguez, J. W. M. Ocampo, y R. M. E. Escobar, «Acondicionamiento del sensor de pH y temperatura para realizar titulaciones potenciométricas», Sci. Tech., vol. XVII, n.o 51, pp. 188-196, 2012.

[30] S. Geetha y S. Gouthami, «Internet of things enabled real time water quality monitoring system», Smart Water, vol. 2, n.o 1, p. 1, jul. 2017, doi: 10.1186/s40713-017-0005-y.

[31] M. Manoj, V. Dhilip Kumar, M. Arif, E.-R. Bulai, P. Bulai, y O. Geman, «State of the Art Techniques for Water Quality Monitoring Systems for Fish Ponds Using IoT and Underwater Sensors: A Review», Sensors, vol. 22, n.o 6, Art. n.o 6, ene. 2022, doi: 10.3390/s22062088.

[32] S. Pasika y S. T. Gandla, «Smart water quality monitoring system with cost-effective using IoT», Heliyon, vol. 6, n.o 7, p. e04096, jul. 2020, doi: 10.1016/j.heliyon.2020.e04096.

[33] C. Mohamed, A. Belaout, y K. Ramdane, «An Arduino-based Water Quality Monitoring System using pH, Temperature, Turbidity, and TDS Sensors», jun. 2023.

[34] A. CREUS, Instrumentation Industrial Edition. Marcombo, 2014.

[35] Y. Villasana, N. Moradi, C. Navas-Cárdenas, y G. S. Patience, «Experimental methods in chemical engineering: pH», Can. J. Chem. Eng., vol. 100, n.o 8, pp. 1703-1717, ago. 2022, doi: 10.1002/cjce.24393.

[36] S. B. Raj, P. H. Prasad, S. Prasath, y A. Moorthy, «Water Quality Monitoring System Using Arduino».

[37] F. Akhter, H. R. Siddiquei, M. E. E. Alahi, y S. C. Mukhopadhyay, «Recent Advancement of the Sensors for Monitoring the Water Quality Parameters in Smart Fisheries Farming», Computers, vol. 10, n.o 3, Art. n.o 3, mar. 2021, doi: 10.3390/computers10030026.

[38] [38] E. T. de Camargo et al., «Low-Cost Water Quality Sensors for IoT: A Systematic Review», Sensors, vol. 23, n.o 9, Art. n.o 9, ene. 2023, doi: 10.3390/s23094424.

[39] [39] J. Hacker, «Assessing the Ability of Arduino-Based Sensor Systems to Monitor Changes in Water Quality», HonorsCollegeTheses, 2023.

[40] [40] W. J. Hong et al., «Water Quality Monitoring with Arduino Based Sensors», Environments, vol. 8, n.o 1, Art. n.o 1, ene. 2021, doi: 10.3390/environments8010006.

[41] [41] U. Ahmed, R. Mumtaz, H. Anwar, S. Mumtaz, y A. M. Qamar, «Water quality monitoring: from conventional to emerging technologies», Water Supply, vol. 20, n.o 1, pp. 28-45, feb. 2020, doi: 10.2166/ws.2019.144.

[42] [42] N. S. Kamaruidzaman y S. Nazahiyah Rahmat, «Water Monitoring System Embedded with Internet of Things (IoT) Device: A Review», IOP Conf. Ser. Earth Environ. Sci., vol. 498, n.o 1, p. 012068, may 2020, doi: 10.1088/1755-1315/498/1/012068.

[43] [43] S. Casans, A. E. Navarro, R. García-Gil, D. Ramírez, y B. Marco, «Red de sensores inteligentes aplicada a la medida de pH y temperatura», Semin. Anu. Automática Electrónica Ind. E Instrum. SAAEI, 2005.

[44] [44] S. Honda et al., «Detachable Flexible ISFET-Based pH Sensor Array with a Flexible Connector», Adv. Electron. Mater., vol. 6, n.o 10, p. 2000583, oct. 2020, doi: 10.1002/aelm.202000583.

[45] [45] Y. R, H. K. S, M. S. M, S. M, L. Pramiee, y A. A. Kumari, «IWQMA: Intelligent Water Quality Management in Aquaculture using IoT Technology», TWIST, vol. 18, n.o 4, Art. n.o 4, dic. 2023.

[46] [46] O. J. Salcedo-Parra y N. G. Agudelo-Cristancho, «Desempeño RSSI de nodos sensores LoRa, BLE y WiFi en un sistema IoT interoperable», Aibi Rev. Investig. Adm. E Ing., vol. 9, n.o 2, pp. 19-32, ago. 2021, doi: 10.15649/2346030X.905.

[47] [47] I. F. Almojela et al., «WatAr: An Arduino-based Drinking Water Quality Monitoring System using Wireless Sensor Network and GSM Module», IEEE REGION 10 CONFERENCE (TENCON), nov. 2020, pp. 550-555. doi: 10.1109/TENCON50793.2020.9293896.

[48] [48] H. A. Mohammed y S. F. Ismail, «Design and implementation of remotely monitoring system for pH level in Baghdad drinking water networks», TELKOMNIKA Telecommun. Comput. Electron. Control, vol. 19, n.o 3, Art. n.o 3, jun. 2021, doi: 10.12928/telkomnika.v19i3.12921.

[49] [49] J. Dhillon, S. Das, N. K. Mohonto, M. Hasan, S. Ahmed, y S. C. Das, «IoT based Water Level Monitoring and Motor Control System», en 2021 4th International Conference on Recent Developments in Control, Automation & Power Engineering (RDCAPE), oct. 2021, pp. 30-34. doi: 10.1109/RDCAPE52977.2021.9633405.

[50] [50] A. R. Braga, J. de C. Rabelo, A. de C. Callado, A. R. da Rocha, B. M. Freitas, y D. G. Gomes, «BeeNotified! A Notification System of Physical Quantities for Beehives Remote Monitoring», Rev. Informática Teórica E Apl., vol. 27, n.o 3, Art. n.o 3, jun. 2020, doi: 10.22456/2175-2745.90724.

[51] C. Feng, J. Yuan, Y. Sun, y J. You, «Design of Water Quality Monitoring System», International Conference on Artificial Intelligence and Computer Engineering (ICAICE), oct. 2020, pp. 264-267. doi: 10.1109/ICAICE51518.2020.00057.

[52] S. Zahoor y S. A. Sofi, «Internet of Things: A Review of Functionality, Applications, Architectures and Challenges», vol. 23, n.o 9, 2021.

[53] R. U. Islam, K. Andersson, y M. S. Hossain, «Heterogeneous wireless sensor networks using CoAP and SMS to predict natural disasters», IEEE Conference on Computer Communications Workshops (INFOCOM WKSHPS), may 2017, pp. 30-35. doi: 10.1109/INFCOMW.2017.8116348.

[54] U. D. Black, Redes de transmisión de datos y proceso distribuido. Ediciones Díaz de Santos, 1987.

[55] D. A. B. Cruz y M. T. S. Rodríguez, «Plan de Negocios de un Localizador de Objetos con Uso de IOT y Aplicación para Android», Universidad Santo Tomás Facultad de Ingeniería Electrónica, Bogotá, 2022.

Author Profile

José de Jesús Moreno Vázquez, he obtained a B. S degree in Electronic Engineering from the Instituto Tecnológico de Minatitlán, Veracruz, México, in 1995. He received the MSc degree from the Centro Nacional de Investigación y Desarrollo Tecnológico National (CENIDET) in 1996 and the Ph. D. degree in Bioengineering from the Universidad Politécnica de Valencia in 2011. He is currently head of research projects in the Department of Electronic Engineering and professor of the Master's Degree in Electronic Engineering. His current interests are digital systems, digital signal processing, bioelectronics, and instrumentation.

Aldo Rafael Sartorius Castellanos, he received the B. S degree in Electromechanical Engineering from the Universidad Veracruzana (UV) in 2000. He received the MSc and Ph. D. degrees in Automatics from the Universidad Central de las Villas (UCLV) in 2002 and 2005, respectively. He currently works as a full-time Professor at the Tecnológico Nacional de México campus, Instituto Tecnológico de Minatitlán (TecNM / ITM) and collaborates as a visiting professor at the Centro de Tecnología Avanzada (CIATEQ). His research lines are focused on the automation and control of electromechanical systems using embedded systems.

Elsa Noemí Palomo Morales, she obtained a B. S degree in Electronic Engineering from the Instituto Tecnológico de Minatitlán, Veracruz, México, in 1988 and the Ph. D. degree in Biolearning from the Universidad Popular Autónoma de Veracruz in 2016. She is currently a professor in the Department of Electronic Engineering and Head of Liaison, as well as President of The Academy of the Electronic Engineering Department.

Marcia Lorena Hernández Nieto, she obtained a B. S degree in Electronic Engineering from the Instituto Tecnológico de Minatitlán, Veracruz, México, in 1992. She received the MSc degree from the Centro Nacional de Investigación y Desarrollo Tecnológico National (CENIDET) in 1994. She is currently a professor in the Department of Electronic Engineering and the Master's Degree in Electronic Engineering. Her areas of interest are in power electronics.

Antonia Zamudio Radilla, obtained her Electronic Engineer title from the Instituto Tecnológico de Minatitlán, Veracruz México in 1996. Master in University Teaching from the Universidad Iberoamericana Golfo Centro, Puebla, México, in 2012. She is currently assigned to the Department of Electronic Engineering. She is a professor of the Master's Degree in Electronic Engineering and the Bachelor's Degree in Electronic Engineering at I.T. from Minatitlán.